Transport in Porous Media manuscript No.
(will be inserted by the editor)

Sensitivity of Travelling Wave Solution to Richards Equation to Soil Material Property Functions

Y. A. Boakye-Ansah · **P. Grassia**

Received: date / Accepted: date

Abstract Richards equation describes water transport in soils, but requires as input, soil material property functions specifically relative hydraulic conductivity and relative diffusivity typically obtained from the soil-water retention curve (SWRC) function (involving capillary suction head). These properties are often expressed via particular functional forms, with different soil types from sandstones to loams represented within those functional forms by a free fitting parameter. Travelling wave solutions (profile of height $\hat{\xi}$ against moisture content Θ) of Richards equation using van Genuchten's form of the soil material property functions diverge to arbitrarily large height close to full saturation. The value of relative diffusivity itself diverges at full saturation owing to a weak singularity in the SWRC. If however soil material property data are sparse near full saturation, evidence for the nature of that divergence may be limited. Here we rescale the relative diffusivity to approach unity at full saturation, removing a singularity from the original van Genuchten SWRC function by constructing a convex hull around it. A piecewise SWRC function results with capillary suction head approaching zero smoothly at full saturation. We use this SWRC with the Brooks-Corey relative hydraulic conductivity to develop a new relative diffusivity function and proceed to solve Richards equation. We obtain logarithmic relationships between height $\hat{\xi}$ and moisture content Θ close to saturation. Predicted $\hat{\xi}$ values are smaller than heights obtained when solving using the original van Genuchten's soil material property functions. Those heights instead exhibit power law behaviour.

1 Introduction

Modelling flow in porous media is important not only in groundwater flow but in many other areas such as suspension dewatering (Aziz et al., 2000; Buscall and White, 1987) and fluid

Y. A. Boakye-Ansah
Present address:Department of Petroleum and Natural Gas Engineering, University of Energy and Natural Resources, Ghana
E-mail: yaw.boakye-ansah@uenr.edu.gh

P. Grassia
Department of Chemical and Process Engineering, University of Strathclyde, James Weir Building, 75 Montrose Street, Glasgow, G1 1XJ, UK
E-mail: paul.grassia@strath.ac.uk

recovery, e.g. oil recovery (Ahmed, 2006; Grassia et al., 2014). Study of this phenomenon requires detailed and careful formulation of the governing equations which depend not only on the fluid, but also on the properties of the porous media in question. In particular, Richards equation (hereafter RE) is the fundamental equation used to describe groundwater flow (Richards, 1931).

In order to solve RE, we require soil material property (hydraulic) functions, namely, capillary suction head, relative hydraulic conductivity (RHC) and relative diffusivity (RD). Using the soil-water retention curve (SWRC) which gives the relationship between capillary suction head and moisture content present in the soil, the latter two functions can also be derived (van Genuchten, 1980). Usually, an analytical SWRC is used with a predictive conductivity model (hereafter PCM) to determine the RHC (van Genuchten, 1980; Assouline, 2001). This RHC is then used with the derivative of capillary suction head to determine the relative diffusivity. Since the SWRC is used to predict these other hydraulic functions, it is important to have a reasonably accurate representation of the retention curve.

A number of functional forms for SWRC are available in literature (Assouline et al., 1998; Brooks and Corey, 1964; Fredlund and Xing, 1994; van Genuchten, 1980). Among those commonly used are the ones proposed by Brooks-Corey (Brooks and Corey, 1964) and van Genuchten (van Genuchten, 1980). The Brooks-Corey SWRC model is described as accurate at low moisture content but less accurate near full saturation (Assouline et al., 1998; Stankovich and Lockington, 1995). Additionally, it goes to a finite capillary suction head value at full saturation, whereas zero capillary suction is expected in that limit. The van Genuchten SWRC model is similar to Brooks-Corey at low saturation but matches field data more accurately at higher saturation than the Brooks-Corey SWRC does (Assouline et al., 1998; Stankovich and Lockington, 1995; Vogel and Cislerova, 1988). It goes to zero suction pressure at full saturation, but at the expense, as we will see, of introducing a singularity near full saturation. Specifically, the derivative of the suction pressure is infinite at full saturation. The van Genuchten model achieves this by introducing an inflection point in the SWRC which is absent in the Brooks-Corey model (Stankovich and Lockington, 1995). In van Genuchten's SWRC, the derivative of the SWRC increases moving in either direction away from the inflection point. We shall focus on the van Genuchten SWRC in this paper. The concern addressed here however is that when one is trying to fit van Genuchten's SWRC to experimental data, unless a significant amount of experimental data are available in the neighbourhood of full saturation, it is uncertain whether the particular singular behaviour of the fitted van Genuchten model predicted in that limit really is an accurate reflection of the true SWRC. In view of that, there is even scope for exploring variants of the SWRC which do not exhibit such singularities.

As mentioned earlier, a so-called predictive conductivity model (hereafter PCM) can be employed with a SWRC function to obtain the relative hydraulic conductivity (RHC) (Assouline and Tartakovsky, 2001; Burdine, 1953; Mualem, 1976; van Genuchten, 1980). The derivation and application of a PCM is discussed further in Appendix A. By definition, the RHC should approach unity as the system approaches full saturation. It is defined as conductivity relative to the conductivity at full saturation. As we see in Appendix A, the singularity in the SWRC is needed to keep the RHC finite at saturation, at least if a PCM is used. Between the two most commonly used PCM, namely the Burdine (1953) and Mualem (1976) models, the Mualem model is claimed to match field data more accurately and is thus more commonly used (Assouline and Tartakovsky, 2001; van Genuchten, 1980). Using the Mualem PCM, the singularity in the SWRC predicts a RHC that goes to unity abruptly, again with a derivative that is singular. Similarly, due to this SWRC singularity, the relative diffusivity (which is obtained as a product of the relative hydraulic conductivity and the derivative of the capillary suction head) diverges at full saturation (Morrow and Harris, 1965), making it more difficult incidentally to attain that saturated state. Another consequence of this (as Appendix A explains) is that, if we alter the SWRC to avoid a singularity at full saturation the PCM fails to converge, we must also alter the conductivity model employed.

As previously deduced (Boakye-Ansah and Grassia, 2021), Richards equation admits travelling wave solutions (profile of height $\hat{\xi}$ against moisture content Θ) using the hydraulic functions given by van Genuchten (1980). These travelling waves were shown to have known asymptotic analytical forms both in the limit of very low ($\Theta \ll 1$) and large ($\Theta \approx 1$) moisture content. The obtained analytical travelling wave solutions show a power law behaviour in these limits. In particular at $\Theta \approx 1$, the travelling wave solution diverges to infinity as a power law due to the behaviour of relative diffusivity at full saturation. Specifically, height $\hat{\xi}$ scales as a negative power of $(1-\Theta)$, the exponent of the power law depending on soil properties. Thus, Θ only approaches full saturation over very large vertical distances, or equivalently at given height $\hat{\xi}$, the system can remain surprisingly far away from full saturation (details in Appendix B).

Previous work (Boakye-Ansah and Grassia, 2021) has shown strong physical and mathematical analogies between foam drainage and Richards equation, foams having a capillary pressure (analogous to the SWRC) and also an analogue of a relative hydraulic conductivity and a relative diffusivity. Unlike the case with Richards equation, these functions do not exhibit singularities in the limit as a foam breaks up into a bubbly liquid (the analogue of what would be considered full saturation in a porous medium). The resulting travelling wave solution for profile of height $\hat{\xi}$ against moisture content Θ no longer has a power law divergence, but rather diverges less strongly, i.e. logarithmically. Near saturation conditions are thereby attained at far more modest heights. An interesting question is whether, in the case of soils with singularities in the SWRC removed, the behaviour will be similar to the original travelling wave solutions for soils, or whether instead they will be more akin to those results for foam drainage.

To summarise, this work seeks to explore the possibility and consequence of removing the singularity from the SWRC function, and to evaluate the impact of this change on the travelling wave solution to Richards equation. We shall explore numerical and approximate asymptotic travelling wave solutions when the singularities for these soil material properties are relaxed. We find that the travelling wave solutions obtained show a logarithmic law in the region of large moisture content as has been obtained for the two foam drainage equation variants in the same limit.

This paper is laid out as follows: in Section 2, we review the fundamental equations that govern fluid flow in unsaturated soils and in foams. We focus on Richards equation and its dimensionless form, and we give the foam drainage equations and corresponding solutions also. In the next section after that, namely Section 3, we analyse the equations used to describe the soil material property functions showing how singularities can be removed by suitably modifying the material properties in the governing equation. If SWRC data are sparse near full saturation, there is limited justification (at least based on curve fitting alone) for selecting the original singular SWRC over the non-singular variants we derive. We present the results and discussion for profile of heights $\hat{\xi}$ vs moisture content Θ in Section 4, and then conclude the paper in Section 5. A key result we will emphasise is that close to saturation, the travelling wave solutions from the modified RE behave more similarly to the foam drainage solutions, than to the original RE ones.

2 Governing Equations

We now present the governing equations that we shall use in this work, namely, Richards equation and foam drainage equation. The travelling wave solutions for foam drainage are available (Boakye-Ansah and Grassia, 2021; Cox et al., 2000; Verbist et al., 1996) and shall thus not be rederived. The solutions are merely quoted in this paper. Later on, we also rescale the Richards equation to match the foam drainage equation by rescaling the relative diffusivity to be unity at full saturation since the foam drainage diffusivities already have that property. This will allow for easier comparison of solutions.

2.1 Foam Drainage Equations

We know from literature that there are two main equations that are used to describe drainage in foams. These are respectively the channel-dominated foam drainage equation (CD FDE) (Verbist et al., 1996; Weaire and Phelan, 1996) and the node-dominated foam drainage equation (ND FDE) (Koehler et al., 1999, 2000), and they differ according to whether dissipation in the foam is assumed to take place in Plateau border (PB) channels or vertex nodes, respectively. The equations are thus given in dimensionless form as

$$\frac{\partial \Theta}{\partial \hat{\tau}} - \frac{\partial}{\partial \hat{\xi}} \cdot \sqrt{\Theta} \frac{\partial \Theta}{\partial \hat{\xi}} - \frac{\partial \Theta^2}{\partial \hat{\xi}} = 0, \tag{1}$$

and

$$\frac{\partial \Theta}{\partial \hat{\tau}} - \frac{\partial}{\partial \hat{\xi}} \cdot \frac{\partial \Theta}{\partial \hat{\xi}} - \frac{\partial \Theta^{3/2}}{\partial \hat{\xi}} = 0, \tag{2}$$

where equations (1) and (2) are respectively the channel-dominated and node-dominated foam drainage equation. Here, $\hat{\tau}$ is a rescaled dimensionless time and $\hat{\xi}$ is a rescaled dimensionless vertical coordinate measured upward. Details of how to make the equations dimensionless can be found in Boakye-Ansah and Grassia (2021). Also, Θ denotes here not the absolute moisture content in the foam, but rather the relative moisture content, relative to the point at which the foams breaks up into a bubbly liquid. By analogy with Section 2.2 presented later on, we observe that the analogous values to relative hydraulic conductivity (Θ^2 & $\Theta^{3/2}$) and relative diffusivity ($\sqrt{\Theta}$ & 1) are known (for CD and ND FDE respectively), and these go to finite unit values when the system reaches full saturation (i.e. $\Theta = 1$). We examine the travelling wave solution $\Theta(\hat{\xi}, \hat{\tau}) = \Theta(\hat{\xi} + \upsilon \hat{\tau})$ for foam drainage, where υ is a dimensionless wave velocity. If we consider $\Theta = 1$ upstream and $\Theta = 0$ downstream, then it is possible to show that $\upsilon = 1$ (both for CD and ND FDE). After taking the first integral (Boakye-Ansah and Grassia, 2021), we can compute the shape of the travelling wave expressed in the form $\hat{\xi}$ vs Θ. We deduce for CD FDE,

$$\mathrm{d}\hat{\xi}/\mathrm{d}\Theta = 1/\left(\sqrt{\Theta}\,(1-\Theta)\right), \tag{3}$$

and for ND FDE,

$$\mathrm{d}\hat{\xi}/\mathrm{d}\Theta = 1/\left(\Theta\,(1-\sqrt{\Theta})\right). \tag{4}$$

Integrating again, we obtain for CD FDE,

$$\hat{\xi} = 2 \operatorname{arctanh} \sqrt{\Theta}, \tag{5}$$

and for ND FDE,

$$\hat{\xi} = 2\log\left(\sqrt{\Theta}/(1-\sqrt{\Theta})\right). \tag{6}$$

Their asymptotic solutions are for CD FDE,

$$\hat{\xi}\Big|_{\Theta \ll 1} \approx 2\sqrt{\Theta}; \qquad \hat{\xi}\Big|_{\Theta \approx 1} \approx \log\left(1/(1-\Theta)\right) + \log 4, \tag{7}$$

while for ND FDE, we deduce

$$\hat{\xi}\Big|_{\Theta \ll 1} \approx \log\,(\Theta); \qquad \hat{\xi}\Big|_{\Theta \approx 1} \approx 2\,\log\,(1/(1-\Theta)) + \log 4, \tag{8}$$

where the terms log 4 in equations (7)–(8) are needed to match with equations (5)–(6). The behaviour in the $\Theta \to 0$ limit are clearly very different ($\hat{\xi} \to 0$ in one case and $\hat{\xi} \to \infty$ in the other), but we focus here on the $\Theta \approx 1$ behaviour. It is clear that the ND FDE predicts a $\hat{\xi}$ roughly twice the CD FDE value.

2.2 Richards Equation

In solving for the Richards equation, we have previously used (Boakye-Ansah and Grassia, 2021) a diffusivity function that diverges at full saturation. Indeed soil-water diffusivity functions that diverge at full saturation are commonly employed to solve Richards equation (Ahuja and Swartzendruber, 1972). This is certainly the case using the van Genuchten (1980) model and it is unavoidable with that model (see Appendix A). Clearly, if diffusivity diverges at full saturation, there is no scope to rescale it to obtain a relative diffusivity that is unity in that limit. This behaviour does not then allow for an equal comparison with foam drainage, neither with the channel-dominated case nor with the node-dominated FDE since their relative diffusivity functions ($\sqrt{\Theta}$ and 1 respectively) go to unity at full saturation. In what follows, we depart from the van Genuchten model in order to formulate a variant of Richards equation with a finite relative diffusivity in the $\Theta \to 1$ limit that allows for a rescaled relative diffusivity (given in Section 3.3) which is equal to 1 when moisture content is unity ($\Theta = 1$). For the moment however, we consider Richards equation as originally formulated.

2.2.1 Rescaling Richards Equation

The moisture-based Richards equation is given as (Philip, 1957; Celia et al., 1990),

$$\partial\theta/\partial t - \nabla \cdot D(\theta)\nabla\theta - \partial K(\theta)/\partial z = 0. \tag{9}$$

Here, θ is volumetric moisture content, t is time, $D(\theta)$ is diffusivity, $K(\theta)$ is hydraulic conductivity and z is depth of infiltration (measured positive upward). The relative/rescaled moisture content which describes the volumetric moisture content θ, is given as

$$\Theta = (\theta - \theta_r)/(\theta_s - \theta_r), \tag{10}$$

where θ_r and θ_s are residual and saturated moisture content respectively.

After suitable nondimensionalization of equation (9), we deduce (details are given in Boakye-Ansah and Grassia (2021))

$$\frac{\partial\Theta}{\partial\tau} - \frac{\partial}{\partial\xi} \cdot D_r(\Theta)\frac{\partial\Theta}{\partial\xi} - \frac{\partial K_r(\Theta)}{\partial\xi} = 0, \tag{11}$$

which is the dimensionless Richards equation. Here τ is dimensionless time, ξ is dimensionless spatial coordinate (measured upwards), $K_r(\Theta)$ is relative hydraulic conductivity and $D_r(\Theta)$ is relative diffusivity. Note that

$$D_r(\Theta) = K_r(\Theta)\,|\mathrm{d}H_+/\mathrm{d}\Theta|\,, \tag{12}$$

where $H_+(\Theta)$ is dimensionless capillary suction head. There are various additional physical effects which can be introduced now (Cuesta et al., 2000; Beliaev and Hassanizadeh, 2001; van Duijn et al., 2018; Mitra and van Duijn, 2019; El Behi-Gornostaeva et al., 2019), such as hysteresis (in which H_+ depends upon whether Θ is increasing or decreasing over time) and dynamic capillarity (in which H_+ depends upon the rate of change of Θ, not just on Θ itself). Here however such effects are neglected and we treat H_+ simply as a function of Θ.

The focus then is just upon the functional form of H_+. More discussion of this functional form of H_+ will be given in Section 3. Strictly speaking, capillary suction head H is negative, but we define $H_+ = -H$ in order to obtain a positive quantity. However, H_+ decreases as Θ increases, so that $\mathrm{d}H_+/\mathrm{d}\Theta$ is negative but its absolute value $|\mathrm{d}H_+/\mathrm{d}\Theta|$ is positive. Here $\lim_{\Theta\to 1} K_r = 1$ by definition. It then follows that $\lim_{\Theta\to 1} D_r = \lim_{\Theta\to 1} |\mathrm{d}H_+/\mathrm{d}\Theta|$.

Even though $\lim_{\Theta\to 1} K_r = 1$ as we have said, making equation (11) directly comparable with the foam drainage equations (3)–(4) is problematic as was alluded to previously, since according to the van Genuchten formula for suction head H_+, it turns out $\lim_{\Theta\to 1} |\mathrm{d}H_+/\mathrm{d}\Theta| \to \infty$. Thus, $\lim_{\Theta\to 1} D_r(\Theta) \to \infty$. As already alluded to, having large diffusivities close to full saturation is common and in fact is a part of the physics of soils (Morrow and Harris, 1965): it implies that liquid is readily drawn away from high saturation regions, such that it is often difficult to reach full saturation, although there are scenarios in which full saturation can be reached even so (van Duijn et al., 2018; Mitra and van Duijn, 2019). In previous work, it has been found that approach to full saturation is very slow when diffusivity is large (Boakye-Ansah and Grassia, 2021): approaching anywhere close to full saturation was found to require very large distances within a soil, or equivalently over a specified distance, soils could remain quite some amount away from full saturation. Having large (i.e. diverging) diffusivities in soils makes it challenging though to carry out a like-for-like comparison between flow of moisture in soils (the present section) and drainage of foams (section 2.1).

We can however resolve this by capping the value of $\mathrm{d}H_+/\mathrm{d}\Theta$ at some value β rather than letting it diverge as van Genuchten would (more details of this in Section 3.3). We then take $D_r = \beta \hat{D}_r$ with $\hat{D}_r$ being a rescaled relative diffusivity. This helps to achieve our aim of making the Richards equation relative diffusivity comparable to the foam drainage relative diffusivity (see Section 3.3), although possibly at the expense of making some modelling errors for soils very close to full saturation. We now choose $\hat{\tau} = \beta^{-1}\tau$ and $\hat{\xi} = \beta^{-1}\xi$. From these definitions and equation (11), we obtain a new dimensionless form for Richards equation,

$$\frac{\partial \Theta}{\partial \hat{\tau}} - \frac{\partial}{\partial \hat{\xi}} \cdot \hat{D}_r(\Theta)\frac{\partial \Theta}{\partial \hat{\xi}} - \frac{\partial K_r(\Theta)}{\partial \hat{\xi}} = 0. \tag{13}$$

This form of Richards equation is scaled to be equivalent to the foam drainage equations (1)–(2) since both relative hydraulic conductivity and relative diffusivity are scaled to become unity at full saturation.

Following from previous derivations, we look for travelling wave solution to Richards equation of the form $\Theta = \Theta(\hat{\xi} + \upsilon\hat{\tau})$. If we impose conditions $\Theta = 1$ upstream, and $\Theta = 0$

downstream, then again $\upsilon = 1$ and the equation governing $\hat{\xi}$ vs Θ turns out to be,

$$\frac{\mathrm{d}\hat{\xi}}{\mathrm{d}\Theta} = \frac{\hat{D}_r(\Theta)}{\Theta - K_r(\Theta)}, \tag{14}$$

upon which we shall base our solutions (and then compare with equations (5)–(6)).

Another way of writing the above equation (upon multiplying through both sides by β) is

$$\frac{\mathrm{d}\xi}{\mathrm{d}\Theta} = \frac{D_r(\Theta)}{\Theta - K_r(\Theta)}. \tag{15}$$

We can now change the variable from Θ to $H = -H_+$. Using equation (12), it follows

$$\frac{\mathrm{d}\xi}{\mathrm{d}H} = \frac{K_r(H)}{\Theta(H) - K_r(H)}, \tag{16}$$

where on the right hand side we have now inverted the expression for capillary suction head into a function of the form $\Theta(H)$, and have also recognised that hydraulic conductivity K_r can be written in the form $K_r = K_r(H)$. This then is a travelling wave equation derived from a so called head-based form, rather than a moisture-based form of Richards equation (Celia et al., 1990). The equation avoids using $D_r(\Theta)$ and hence, even without imposing a cap on diffusivity, avoids dealing with any awkward divergence in $D_r(\Theta)$ as full saturation is approached. However, whereas the original variable Θ covered the domain $0 \leq \Theta \leq 1$, the values of H now cover the domain $-\infty < H \leq 0$. It is unclear therefore how to compare such a solution for ξ vs H in the case of soils with the solutions for the foam drainage equations, which were not specifically formulated to cover the exact same domain of capillary suction pressures. It is for this reason that we prefer in the present paper to work with equation (14) in spite of the capped diffusivities.

The solutions to Richards equation will be studied in further detail in Section 4. Before that however, we need to supply the soil material property functions $K_r(\Theta)$ and $\hat{D}_r(\Theta)$.

3 Soil Material Property Functions

In this section, we consider the equations that we shall employ in this paper to model the properties of the porous media. We first study the capillary suction head by formulating a new equation based on the existing van Genuchten one. The new equation goes smoothly to zero suction at full saturation and is realised by constructing a convex hull around the original van Genuchten capillary suction head. We subsequently focus on the relative hydraulic conductivity model we shall use, and thence develop the relative diffusivity function.

Throughout, we work in terms of dimensionless variables in a similar fashion to what was done by Boakye-Ansah and Grassia (2021): the conversions between dimensional and dimensionless variables are again detailed by Boakye-Ansah and Grassia (2021).

3.1 Capillary Suction Head

Brooks and Corey (1964) proposed a SWRC (head) function given as

$$H_+ = \Theta^{-1/\lambda}, \tag{17}$$

where λ is the pore-size distribution parameter. This particular SWRC is reported to be very accurate in the case of dry systems ($\Theta \ll 1$) but less so as $\Theta \to 1$ (Assouline et al., 1998; Stankovich and Lockington, 1995; Vogel and Cislerova, 1988). Note in particular that this function does not go to zero ($H_+ \neq 0$) as $\Theta \to 1$. To address this van Genuchten (1980) modified equation (17) by choosing a formula that agrees with it in the dry ($\Theta \ll 1$) limit but which has $H_+ \to 0$ when $\Theta \to 1$ albeit with an abrupt approach to $H_+ \to 0$. The van Genuchten (1980) SWRC function has been described as performing better than the Brooks-Corey SWRC function near full saturation (Assouline et al., 1998). The van Genuchten SWRC function is given as

$$\Theta = \left[1/(1+H_+^n)\right]^m; \qquad H_+ = (\Theta^{-1/m}-1)^{1/n}; \qquad H_+ = (\Theta^{-1/m}-1)^{1-m}, \tag{18}$$

where in the first instance m and n are independent parameters but for the Mualem predictive conductivity model (PCM) (van Genuchten, 1980), $m = 1-1/n$ (and the Brooks-Corey λ can be identified with $\lambda = m/(1-m)$). The parameter m can be considered to determine the type of soils, with $m \to 1$ corresponding to sandstone and significantly smaller m (down to about $m \approx 1/2$) corresponding to clayey loams. Appendix A discusses how m influences pore size distribution, particularly in the limit of large pores. The Mualem relation, namely $m = 1-1/n$ used by van Genuchten (1980), fits experimental data less well than keeping m and n general, but since a general form leads to more complicated expressions for material property functions (van Genuchten and Nielsen, 1985), we choose to retain $m = 1-1/n$ as per van Genuchten (1980).

Note that, the derivative of equation (18) diverges as $\Theta \to 1$. In this limit equation (18) can be written as

$$H_+ \approx ((1-\Theta)/m)^{1-m}, \tag{19}$$

so that

$$\left|\frac{\mathrm{d}H_+}{\mathrm{d}\Theta}\right| \approx \frac{(1-m)}{m^{1-m}}(1-\Theta)^{-m}. \tag{20}$$

If the data that one is using to fit the H_+ vs Θ profile comes primarily from the dry region ($\Theta \ll 1$), it may be difficult to distinguish the Brooks-Corey head function from the van Genuchten head function. Under these circumstances, it may also be difficult to decide whether the details of how the van Genuchten head function approaches zero in the $\Theta \to 1$ limit are correct. Indeed, it may even be difficult to decide whether the SWRC/head function really exhibits a singular behaviour approaching full saturation. Alternatives to equation (18) are therefore worth exploring.

3.1.1 Developing New Head Function

We can identify a point at which equation (18) definitely differs from equation (19), namely an inflection point at which equation (18) admits $\mathrm{d}^2H_+/\mathrm{d}\Theta^2 = 0$, whereas equation (19) never has an inflection point. We identify the inflection point of equation (18) by setting a double differential to zero as

$$\frac{\mathrm{d}^2H_+}{\mathrm{d}\Theta^2} = \frac{(1+m)(1-m)}{m^2}\frac{(\Theta^{-1/m}-1)^{-m}}{\Theta^{1/m+2}} - \frac{(1-m)}{m}\frac{(\Theta^{-1/m}-1)^{-1-m}}{\Theta^{2/m+2}} = 0, \tag{21}$$

for which we obtain

$$\Theta_{\text{infl}} = (1+m)^{-m}, \tag{22}$$

the value of which is given for different soils in Table 1.

As alluded to above, this inflection point in the van Genuchten SWRC equation (18) indicates a clear departure from the Brooks-Corey SWRC equation (17). It marks a point where $|\mathrm{d}H_+/\mathrm{d}\Theta|$ in the SWRC stops decreasing and starts increasing again. The Brooks-Corey SWRC by contrast has a $|\mathrm{d}H_+/\mathrm{d}\Theta|$ that decreases monotonically. If the parameter m in the van Genuchten SWRC has been estimated based on fitting to data with $\Theta < \Theta_{\mathrm{infl}}$ it becomes very difficult to distinguish the van Genuchten SWRC from the Brooks-Corey SWRC. In a situation like that, we can modify the van Genuchten SWRC by constructing a convex hull around it. The convex hull will agree with the van Genuchten SWRC for $\Theta \ll 1$, but with instead $H_+ \to 0$ as $\Theta \to 1$, albeit now having $|\mathrm{d}H_+/\mathrm{d}\Theta|$ being a monotonically decreasing function as Θ increases (hence, no inflection point). If available data for constructing the SWRC tend to be weighted towards small Θ, there is little evidence to support choosing the original van Genuchten SWRC over the convex hull variant.

The convex hull can be constructed in a (Θ, H_+) plot, by finding a so-called point of tangency Θ_{t}, and drawing a straight line from $(\Theta_{\mathrm{t}}, H_+(\Theta_{\mathrm{t}}))$ to $(1,0)$. The value of Θ_{t} is less than Θ_{infl} and satisfies

$$1-\Theta_{\mathrm{t}} = \frac{H_+(\Theta_{\mathrm{t}})}{|\mathrm{d}H_+/\mathrm{d}\Theta|_{\Theta=\Theta_{\mathrm{t}}}}, \tag{23}$$

where Θ_{t} is the value of Θ at tangency for each profile with different m (different soil type). We obtain

$$1-\Theta_{\mathrm{t}} = \frac{m}{(1-m)}\,\frac{(\Theta_{\mathrm{t}}^{-1/m}-1)}{\Theta_{\mathrm{t}}^{-(1+1/m)}}; \qquad \Theta_{\mathrm{t}} = \frac{1-m}{1-m\Theta_{\mathrm{t}}^{1/m}}, \tag{24}$$

after some algebra. The exact value for Θ_{t} for each m is obtained via a Newton-Raphson method, and it markedly decreases as $m \to 1$. Table 1 gives the Θ_{t} values for three different soil types. Note that $\Theta_{\mathrm{t}} < \Theta_{\mathrm{infl}}$ always. Having identified Θ_{t}, we define the new (piecewise) head function as

$$H_{+(\mathrm{new})}(\Theta,m) = \begin{cases} H_+(\Theta), & \text{if } \Theta \le \Theta_{\mathrm{t}} \\ H_+(\Theta)_{\Theta=\Theta_{\mathrm{t}}} - |\mathrm{d}H_+/\mathrm{d}\Theta|_{\Theta=\Theta_{\mathrm{t}}}(\Theta-\Theta_{\mathrm{t}}), & \text{if } \Theta > \Theta_{\mathrm{t}}. \end{cases} \tag{25}$$

Substituting equation (18) into equation (25), we obtain

$$H_{+(\mathrm{new})}(\Theta,m) = \begin{cases} (\Theta^{-1/m}-1)^{1-m}, & \text{if } \Theta \le \Theta_{\mathrm{t}} \\ (\Theta_{\mathrm{t}}^{-1/m}-1)^{1-m} - \left|\dfrac{(1-m)}{m}\cdot\dfrac{(\Theta_{\mathrm{t}}^{-1/m}-1)^{-m}}{\Theta_{\mathrm{t}}^{1+1/m}}\right|(\Theta-\Theta_{\mathrm{t}}), & \text{if } \Theta > \Theta_{\mathrm{t}}, \end{cases} \tag{26}$$

which can also be presented as

$$H_{+(\mathrm{new})}(\Theta,m) = \begin{cases} (\Theta^{-1/m}-1)^{1-m}, & \text{if } \Theta < \Theta_{\mathrm{t}} \\ \left|\dfrac{(1-m)}{m}\,\dfrac{(\Theta_{\mathrm{t}}^{-1/m}-1)^{-m}}{\Theta_{\mathrm{t}}^{1+1/m}}\right|(1-\Theta), & \text{if } \Theta > \Theta_{\mathrm{t}}. \end{cases} \tag{27}$$

Fig. 1 shows a profile of equations (18) and (26). In contrast with equation (18), by construction equation (26) goes smoothly to zero at full saturation. Additionally, as anticipated

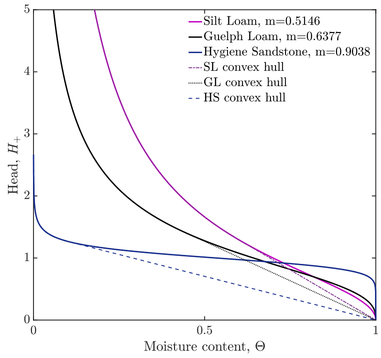

(a)

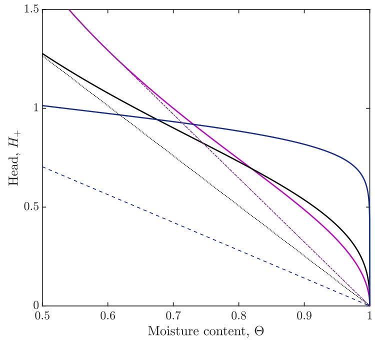

(b)

Fig. 1 Capillary suction head equation (26) profile for three soil samples. The solid lines are plotted using equation (18) whereas the thinner dashed or dotted lines represent those from equation (27). The profile in (a) covers the entire moisture content range while (b) is a zoomed in view near $\Theta \to 1$.

there is no inflection point in this latter equation. Instead, $|\mathrm{d}H_+/\mathrm{d}\Theta|$ decreases monotonically until Θ_t after which it remains fixed. Indeed

$$\left|\frac{\mathrm{d}H_{+(\mathrm{new})}}{\mathrm{d}\Theta}\right| = \begin{cases} \dfrac{(1-m)}{m}\dfrac{(\Theta^{-1/m}-1)^{-m}}{\Theta^{1+1/m}}, & \text{if } \Theta \le \Theta_\mathrm{t} \\[2ex] \dfrac{(1-m)}{m}\dfrac{(\Theta_\mathrm{t}^{-1/m}-1)^{-m}}{\Theta_\mathrm{t}^{1+1/m}}, & \text{if } \Theta > \Theta_\mathrm{t}. \end{cases} \tag{28}$$

Note that although equations (25)–(26) clearly give a different function from equation (18) by introducing a convex hull, we have not introduced any additional free-fitting parameters in equations (25)–(26). The parameter Θ_t is a well defined function of m, not a free parameter. Thus equations (25)–(26) can be viewed as a variant of equation (18) that approaches $H_+ \to 0$ smoothly as $\Theta \to 1$ but which does not contain any additional fitting parameters. Not introducing new parameters was the rationale for using a convex hull here rather than some other variant of the original van Genuchten SWRC.

In the various calculations that follow, we use the function $H_{+(\mathrm{new})}$ exclusively instead of the original H_+. For compactness of notation, we now start to denote this simply by H_+.

Table 1 Soil-specific properties of the three example soils. Values of m are reported in van Genuchten (1980).

Soil	m	Θ_infl	Θ_t	$\lvert\mathrm{d}H_+/\mathrm{d}\Theta\rvert_{\Theta=\Theta_\mathrm{t}}$	c_m	$\hat{c}_m$
Silt Loam	0.5146	0.8076	0.5996	3.2330	0.2918	0.1194
Guelph Loam	0.6377	0.7301	0.4395	2.5327	0.2243	0.1085
Hygiene Sandstone	0.9038	0.5588	0.1039	1.4085	0.0759	0.0471

3.2 Relative Hydraulic Conductivity

The relative hydraulic conductivity (RHC) of porous media is used to describe the relationship between unsaturated hydraulic conductivity and moisture content (Assouline and Or, 2013; Or and Assouline, 2013). It is required for formulation of Richards equation (RE) describing unsaturated flow in soils. RHC may be obtained experimentally but this is tedious, time consuming and expensive (Assouline, 2001; Assouline et al., 1998; Or and Assouline, 2011). Thus, a model or mathematical function that can predict RHC is usually employed (Assouline, 2001). One such model is the predictive conductivity model (PCM). The way in which a PCM converts a H_+ vs Θ profile into a K_r vs Θ is detailed in Appendix A. A specific RHC is obtained by inserting a particular soil-water retention curve SWRC function in this PCM. The theory underlying these PCMs involves a number of assumptions which are never perfectly accurate, so whilst the PCM is often useful, it does not provide an exact representation of K_r vs Θ (Or and Assouline, 2013; van Genuchten and Nielsen, 1985; Vogel and Cislerova, 1988). Thus, even deploying a PCM it is not always possible to obtain RHC which closely match field data (Or and Assouline, 2011; Stankovich and Lockington, 1995; van Genuchten and Nielsen, 1985) making it problematic to rely on the PCM formulation (Vogel and Cislerova, 1988) to give values for RHC in any soil study.

Since K_r is a *relative* hydraulic conductivity (i.e. relative to full saturation), we expect that $K_r \to 1$ as $\Theta \to 1$. For a H_+ vs Θ model that fails to fall to zero at full saturation, it turns out that $K_r \to 1$ in a non-singular fashion. By contrast, for a H_+ vs Θ model that falls to zero at full saturation but does so abruptly (i.e. $|\mathrm{d}H_+/\mathrm{d}\Theta| \to \infty$ at $\Theta \to 1$), K_r still manages to reach unity at full saturation but has a singularity $\mathrm{d}K_r/\mathrm{d}\Theta \to \infty$ as $\Theta \to 1$ (van Genuchten, 1980). However, for a H_+ vs Θ model, such as we study here, that approaches zero smoothly (with finite $\mathrm{d}H_+/\mathrm{d}\Theta$ as $\Theta \to 1$ and $H_+ \to 0$), it turns out that the PCM does not converge. The issue (as explained in the appendix) is that almost all the flow at full saturation is through the largest pores, meaning that slightly below saturation, where these largest pores are no longer filled with liquid, the flow is in relative terms much smaller than at full saturation. The PCM then predicts negligible flow except at full saturation.

In other words, the hydraulic conductivity is so strongly weighted to the largest pores that the computation is sensitive to the largest pore size in a given sample. Convergence in the PCM would be obtained when one has hardly any pore space in the largest pores, or equivalently hardly any pore space in the pores with the smallest capillary suction i.e. $|\mathrm{d}\Theta/\mathrm{d}H_+| \to 0$ as $1/H_+ \to \infty$, or $|\mathrm{d}H_+/\mathrm{d}\Theta| \to \infty$ as $H_+ \to 0$. This is however not the case when equation (26) is used.

To summarise, given the convex hull SWRC in equation (26), we find that using the Mualem PCM yields equations for RHC which do not converge. Thus, we are unable to use the PCM to obtain an RHC expression using the head function we have derived via the convex hull. To avoid these issues, we abandon the PCM for our convex hull head function and employ instead a RHC equation that does not exhibit singular behaviour near full saturation. Specifically, we use the Brooks and Corey RHC (Brooks and Corey, 1964). We use this RHC function in the interest of simplicity (van Genuchten and Nielsen, 1985; Vogel and Cislerova, 1988) and also because it follows a similar pattern to what is seen in the FDE, namely a power law function of saturation albeit with different exponents in the power law between the FDE and RE. It is given as

$$K_r(\Theta) = \Theta^{5/2+2/\lambda} = \Theta^{1/2+2/m}, \tag{29}$$

where $\lambda = m/(1-m)$. This profile is shown in Fig. 2. In addition to this, the RHC for the two foam drainage variants (Koehler et al., 1999, 2000; Verbist and Weaire, 1994; Verbist et al., 1996; Weaire and Phelan, 1996) are also plotted (Θ^2 and $\Theta^{3/2}$ respectively for channel- and node-dominated FDE). What we notice is that RHC for soils tends to be less than that for foam.

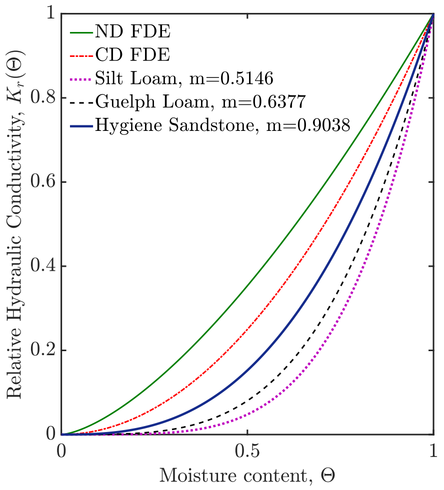

Fig. 2 Plot of RHC profile for three soil samples based on equation (29) and the two FDE variants. The analogous RHC values for channel-dominated FDE (equation (1)) and node-dominated FDE (equation (2)) are Θ^2 and $\Theta^{3/2}$ respectively.

3.3 Relative Diffusivity

In what follows, we develop a rescaled relative diffusivity (RD) function that goes to unity when moisture content approaches unity at full saturation, which matches the behaviour within the two foam drainage equations (FDEs), thereby allowing for a "fairer" comparison between soils and foams. Once the SWRC and RHC are defined, these two soil material functions are used to determine relative diffusivity (RD) (van Genuchten, 1980). This can be accomplished using equation (12). We therefore first define the RD using our newly defined head function equation (26) and the Brooks and Corey (1964) RHC functions equation (29) as

$$D_r(\Theta) = \begin{cases} \dfrac{(1-m)}{m} \cdot \dfrac{\Theta^{1/m-1/2}}{(\Theta^{-1/m}-1)^m}, & \text{if } \Theta \leq \Theta_\mathrm{t} \\[2ex] \left[\dfrac{(1-m)}{m} \cdot \dfrac{(\Theta_t^{-1/m}-1)^{-m}}{\Theta_\mathrm{t}^{1+1/m}}\right] \Theta^{1/2+2/m}, & \text{if } \Theta > \Theta_\mathrm{t}. \end{cases} \tag{30}$$

We then obtain a rescaled $\hat{D}_r(\Theta)$ by dividing both parts of the equation (30) by β defined as the (fixed) value of $|\mathrm{d}H_+/\mathrm{d}\Theta|$ for $\Theta > \Theta_\mathrm{t}$ according to equation (28). That this is the $\Theta \to 1$ limit of D_r follows from equation (12) remembering from (29) that $K_r \to 1$ as $\Theta \to 1$. Hence,

$\hat{D}_r(\Theta)$ is given below as,

$$\hat{D}_r(\Theta) = \begin{cases} \Theta_t^{1+1/m} \cdot (\Theta_t^{-1/m} - 1)^m \dfrac{\Theta^{1/m-1/2}}{(\Theta^{-1/m} - 1)^m}, & \text{if } \Theta \le \Theta_t \\ \Theta^{1/2+2/m}, & \text{if } \Theta > \Theta_t. \end{cases} \tag{31}$$

The prefactor in second part of equation (30) has been scaled out when $\Theta > \Theta_t$ in this new formula for the relative diffusivity. Meanwhile, the prefactor of the first part of equation (31) which hereafter we denote c_m decreases as $m \to 1$ as shown in Table 1. Equation (31) is shown in Fig. 3.

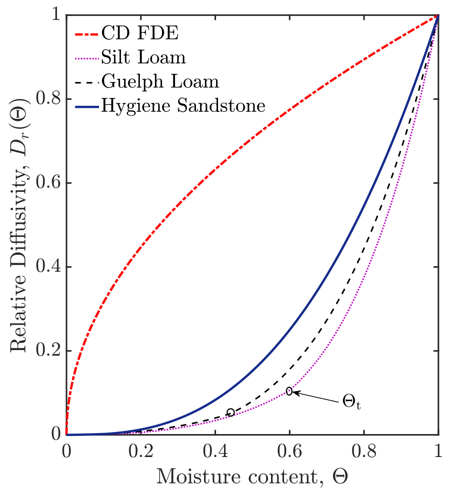

Fig. 3 Relative diffusivity profiles for three soil samples based on (29) and channel-dominated foam drainage. The solution for node-dominated foam drainage is identically unity for all values of Θ and is thus not displayed. In the case of soils, the slope of $\hat{D}_r$ is discontinuous at Θ_t although $\hat{D}_r$ is continuous. In the case of hygiene sandstone, the change in slope is not shown explicitly, as Θ_t is then quite a small value, and the change in slope is difficult to see.

From Fig. 3, we observe that by design when $\Theta = 1$, we have $\hat{D}_r(\Theta) = 1$. We compare the profile of relative diffusivity for three soil samples, and the channel-dominated foam drainage in this plot. The node-dominated profile is not shown as it is identically unity at all values of Θ. The soils (especially loams and particularly Silt Loam, $\Theta_t = 0.5996$) tend to show an observable kink in $\hat{D}_r$ when $\Theta = \Theta_t$. Even though $\mathrm{d}H_+/\mathrm{d}\Theta$ and hence $\hat{D}_r$ are continuous at Θ_t, the values of $\mathrm{d}^2H_+/\mathrm{d}\Theta^2$ and hence $\mathrm{d}\hat{D}_r/\mathrm{d}\Theta$ are not.

This new format rescaled relative diffusivity $\hat{D}_r(\Theta)$ will be used in Section 4 to obtain the travelling wave solution for Richards equation (32).

4 Results: Solution to Richards Equation

We solve for the travelling wave solution to Richards equation for different soil types using the known Brooks-Corey RHC function equation (29) and the modified relative diffusivity function equation (31). From equation (14), we obtain the following expressions,

$$\hat{\xi} = \begin{cases} \Theta_t^{1+1/m} \cdot (\Theta_t^{-1/m} - 1)^m \displaystyle\int_0^{\Theta} \frac{\Theta^{1/m-1/2}}{(\Theta^{-1/m}-1)^m(\Theta - \Theta^{1/2+2/m})} \mathrm{d}\Theta, & \text{if } \Theta \leq \Theta_t \\ \displaystyle\int_{\Theta_t}^{\Theta} \frac{\Theta^{1/2+2/m}}{\Theta - \Theta^{1/2+2/m}} \mathrm{d}\Theta + \hat{\xi}(\Theta_t), & \text{if } \Theta > \Theta_t \,. \end{cases} \tag{32}$$

These integrals cannot be solved analytically, hence, we employ Simpson's rule to obtain numerical solutions, similar to what was done in Boakye-Ansah and Grassia (2021). The solution for different soil types are shown in a profile in Fig. 4 for each soil type. Additionally, the profiles of channel- and node-dominated foam drainage are also shown.

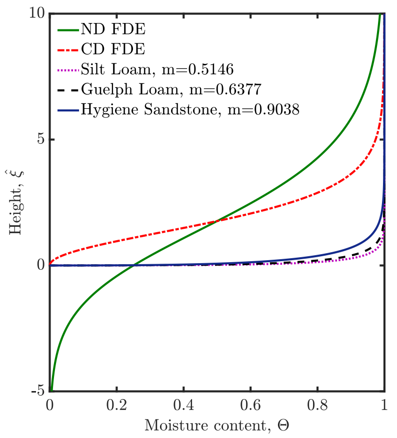

Fig. 4 Profile of numerical travelling wave solution (using Simpson's rule) to equation (32) for three soil samples.

We see that the behaviours both as $\Theta \to 0$ and $\Theta \approx 1$ are very different between foams and soils. The $\hat{\xi}$ values in soils are very slow to increase when $\Theta \ll 1$, and (at least when soil diffusivities are capped as we have assumed here) the increase in $\hat{\xi}$ at $\Theta \to 1$ is also somewhat slower compared to foam (in other words full saturation is approached at a more modest height). These limiting cases are discussed next.

4.1 Asymptotic Behaviour of Solutions

Although analytic solutions to equation (32) are not available in general, it is possible to study analytically how the solution to Richards equation behaves in the limit of small or large Θ. We deduce that the Richards equation travelling wave equation (14) approaches

$$\frac{\mathrm{d}\hat{\xi}}{\mathrm{d}\Theta} \approx \begin{cases} \hat{D}_r(\Theta)/\Theta, & \text{if } \Theta \ll 1, \\ \dfrac{\hat{D}_r(1)}{(1-\Theta)(K_r'(1)-1)}, & \text{if } \Theta \approx 1, \end{cases} \tag{33}$$

where $K_r'(1)$ here denotes $\mathrm{d}K_r/\mathrm{d}\Theta|_{\Theta=1}$.

For $\Theta \ll 1$, from equation (31), we obtain for $\hat{D}_r(\Theta)/\Theta \approx c_m \Theta^{1/m-1/2}$ where as was mentioned earlier $c_m = \Theta_t^{1+1/m} \cdot (\Theta_t^{-1/m} - 1)^m$. Meanwhile, the relative diffusivity $\hat{D}_r(1) \equiv \lim_{\Theta\to 1} \hat{D}_r(\Theta)$ equals unity, whereas the denominator of the second part of equation (33) has been obtained via Taylor series expansion in the $\Theta \approx 1$ limit. Note that $K_r'(1)$ equals $(4+m)/(2m)$ and decreases monotonically as $m \to 1$. Hence,

$$\frac{\mathrm{d}\hat{\xi}}{\mathrm{d}\Theta} \approx \begin{cases} c_m \cdot \Theta^{1/m-1/2}, & \text{if } \Theta \ll 1 \\ 2m/\left((4-m)(1-\Theta)\right), & \text{if } \Theta \approx 1. \end{cases} \tag{34}$$

Integrating equation (34), we obtain

$$\hat{\xi}(\Theta) \approx \begin{cases} \hat{c}_m \cdot \Theta^{1/2+1/m}, & \text{if } \Theta \ll 1 \\ (2m/(4-m)) \cdot \log\left(1/(1-\Theta)\right) + \tilde{c}_2, & \text{if } \Theta \approx 1. \end{cases} \tag{35}$$

where $\hat{c}_m = c_m \cdot 2m/(2+m)$, this value being reported in Table 1 and $\tilde{c}_2$ is a value that can be obtained by matching to the solution of equation (32) via Simpson's rule to an arbitrary Θ value ($\Theta = 0.9$, say) in that limit.

In the dry limit ($\Theta \ll 1$), we observe that the asymptotic approximation exhibits a power law behaviour. This power law behaviour is no different from what was observed in Boakye-Ansah and Grassia (2021) except for having a different prefactor owing to replacing D_r by $\hat{D}_r$. On the contrary, the large Θ behaviour is very different from what was found in Boakye-Ansah and Grassia (2021) being not a power law but rather a logarithmic law instead. Specifically, $\hat{\xi}$ exhibits a logarithmic law behaviour in the limit where $\Theta \to 1$. This then is a manifestation of the convex hull SWRC that we have employed here, not necessarily capturing all the physics of soils close to full saturation. The logarithmic law found here approaches close to full saturation even at comparatively modest $\hat{\xi}$, whereas the power law solutions of Boakye-Ansah and Grassia (2021) using the original SWRC need larger distances to approach close to full saturation, i.e. the approach to full saturation is rather more difficult to achieve in that case (see Appendix B).

The foam drainage equations also exhibit logarithmic behaviour in these limits, but with a different prefactor multiplying the logarithm, 2 for the ND FDE (equation (4)), 1 for the CD FDE (equation (3)), and $2m/(4-m)$ for soils with $m < 1$ here. Clearly, the $\hat{\xi}$ values predicted for soils are less than those for the FDE.

Fig. 5 shows a comparison of the numerical solution to equation (32) and its analytical solutions in equation (35). We observe from these profiles that the analytical solutions in Fig. 5(a) are slight overestimates as $m \to 1$ although it must be stated that the scale of the graph is very small (on the order of 10^{-3}) indicating that $\hat{\xi}$ increases only very slowly with Θ for small $\Theta \ll 1$. The approximation for Silt Loam ($m = 0.5146$) is very accurate. Note also that increasing m increases $\hat{\xi}$ monotonically in Fig. 5(a). This monotonicity was not seen uniformly in Boakye-Ansah and Grassia (2021) because of the different way in which prefactors depended on m in the scaling used there.

Likewise in Fig. 5(b), the profiles for $\hat{\xi}$ are overestimated by the $\Theta \approx 1$ asymptotic formulae for all m values, but these overestimations are small in relative terms for each m. The difference between numerical and asymptotic analytical solutions is far less significant than the difference between soils samples and foam drainage in Fig. 4. The solutions

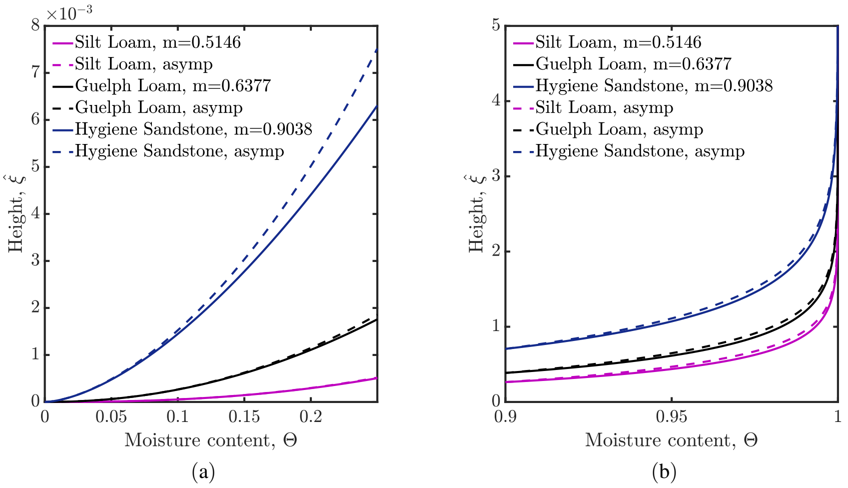

Fig. 5 Profiles of numerical and asymptotic travelling wave solutions to Richards equation in the limit (a) $\Theta \ll 1$, (b) $\Theta \approx 1$. The numerical solutions are the solid lines while the approximate analytical ones are the dashed lines.

show a slower growth in $\hat{\xi}$ in soil than foam as shown in Fig. 4 (whereas with the original SWRC, RHC and RD, the growth was as mentioned like a power law, not a logarithm and hence was much more rapid: see Boakye-Ansah and Grassia (2021) and see also Appendix B). This then indicates an important qualitative change in the travelling wave solution as our original SWRC is replaced by a convex hull SWRC. With the original SWRC, Boakye-Ansah and Grassia (2021) found heights attained for soils to be much larger than for foam. Here however, the foams attain greater heights $\hat{\xi}$ than the soils at given Θ.

The logarithmic law (equation (35)) obtained here for the shape of the travelling wave profile close to full saturation is actually unsurprising. We are using Brooks-Corey type RHC, $K_r = \Theta^{1/2+2/m}$ (defined here without applying any PCM) but a monotonically decreasing $|\mathrm{d}H_+/\mathrm{d}\Theta|$ (obtained here via applying convex hull to the van Genuchten-Mualem SWRC). Qualitatively however this is similar to using a Brooks-Corey RHC along with a Brooks-Corey SWRC $H_+ = \Theta^{-(1-m)/m}$ (the latter also gives a monotonically decreasing $|\mathrm{d}H_+/\mathrm{d}\Theta|$, and leads to $\hat{D}_r = \Theta^{1/2+1/m}$). Although the Brooks-Corey SWRC clearly does not give vanishing head at full saturation, modifying it to $H_+ = -1 + \Theta^{-(1-m)/m}$ (whilst keeping the RHC unchanged) does give vanishing head in that limit and moreover (like the aforementioned convex hull SWRC) still captures the correct power law SWRC behaviour for dry soils such that $\Theta \ll 1$. The above mentioned change in H_+ (introducing an additive constant) has no effect whatsoever on $|\mathrm{d}H_+/\mathrm{d}\Theta|$, hence no effect whatsoever on $\hat{D}_r(\Theta)$, nor on $\hat{\xi}$ vs Θ, which remains unchanged from the Brooks-Corey case. However these Brooks-Corey type formulae (i.e. power laws for $K_r(\Theta)$ and $\hat{D}_r(\Theta)$ in terms of Θ) qualitatively are the same as what is found for channel- or node-dominated foam drainage (again $K_r(\Theta)$ and $\hat{D}_r(\Theta)$ are power laws, just with different powers). Since the foam drainage cases lead to logarithmic $\hat{\xi}$ vs Θ behaviour near saturation (see equations (7)–(8)), it is unsurprising that the Brooks-Corey predictions for soils do so also. Moreover since $\hat{D}_r(1) = 1$ regardless of whether we use a Brooks-Corey SWRC or a convex hull constructed around a van Genuchten SWRC, and since the $K_r(\Theta)$ we use is the same in either case, it follows that equation (33) remains unchanged near $\Theta \approx 1$. The $\Theta \to 1$ prediction of equation (35) is therefore exactly the same as what a Brooks-Corey model would predict.

5 Conclusion

We have considered the travelling wave solution for Richards equation using a modified relative diffusivity function that goes to unity smoothly at full saturation, and a relative hydraulic conductivity function that goes to unity smoothly in the same limit. Here we achieved this by employing a new capillary suction head expression for unsaturated soils constructing a convex hull around the existing van Genuchten SWRC. Our head expression goes to zero smoothly at full saturation for all soil types. This is in contrast to the Brooks-Corey SWRC which does not go to zero, and the van Genuchten SWRC which goes to zero but does so abruptly in a singular fashion. If data used to estimate the SWRC are weighted towards the dry limit, it may be difficult to distinguish these different SWRC, but the predictions they make in the wet limit are very different. We also note that with our chosen convex hull SWRC, we used a Brooks-Corey RHC rather than a PCM, which would not have converged. Employing a Brooks-Corey RHC is compatible in any case with the approach in the foam drainage equation. The solutions of Richards equation were obtained via Simpson's rule, while asymptotic analytical solutions were also derived for very low moisture content ($\Theta \ll 1$), and systems near full saturation ($\Theta \approx 1$).

We found that for the soils, using these modified material properties, we obtain travelling wave solutions $\hat{\xi}$ vs Θ that follow a logarithmic law as in foam drainage as $\Theta \to 1$. The foam heights $\hat{\xi}$ for a given saturation Θ are however larger than those for the soil solutions. Moreover, clayey soils (smaller values of parameter m) attain even lower heights than porous sandstones (m close to unity). The previous Richards equation solutions (Boakye-Ansah and Grassia, 2021) that were obtained without rescaling the relative diffusivity to unity at full saturation reached even larger heights as $\Theta \to 1$. These diverged as a power law rather than logarithmically and were therefore even larger than the foam drainage solutions. We infer then that generally, depending on the scaling of relative diffusivity near full saturation, we may obtain either power law or logarithmic law travelling wave solutions to Richards equation. Changing the nature of the SWRC close to full saturation thereby changes the nature of the travelling wave close to full saturation also.

References

Ahmed T (2006) Reservoir Engineering Handbook, 2nd edn. Elsevier

Ahuja LR, Swartzendruber D (1972) An improved form of soil-water diffusivity function 1. Soil Science Society of America Journal 36(1):9–14

Assouline S (2001) A model for soil relative hydraulic conductivity based on the water retention characteristic curve. Water Resources Research 37(2):265–271

Assouline S, Or D (2013) Conceptual and parametric representation of soil hydraulic properties: A review. Vadose Zone Journal 12(4)

Assouline S, Tartakovsky DM (2001) Unsaturated hydraulic conductivity function based on a soil fragmentation process. Water Resources Research 37(5):1309–1312

Assouline S, Tessier D, Bruand A (1998) A conceptual model of the soil water retention curve. Water Resources Research 34(2):223–231

Aziz AA, De Kretser RG, Dixon DR, Scales PJ (2000) The characterisation of slurry dewatering. Water Science and technology 41(8):9–16

Beliaev AY, Hassanizadeh SM (2001) A theoretical model of hysteresis and dynamic effects in the capillary relation for two-phase flow in porous media. Transport in Porous Media 43:487–510

Boakye-Ansah YA, Grassia P (2021) Comparing and contrasting travelling wave behaviour for groundwater flow and foam drainage. Transport in Porous Media 137(1):255–280

Brooks RH, Corey AT (1966) Properties of porous media affecting fluid flow. Journal of the Irrigation and Drainage Division 92(2):61–90

Brooks RH, Corey T (1964) Hydraulic properties of porous media. Hydrology Papers, Colorado State University 24

Burdine NT (1953) Relative permeability calculations from pore size distribution data. Journal of Petroleum Technology 5(03):71–78

Buscall R, White LR (1987) The consolidation of concentrated suspensions. part 1. — The theory of sedimentation. Journal of the Chemical Society, Faraday Transactions 1: Physical Chemistry in Condensed Phases 83(3):873–891

Celia MA, Bouloutas ET, Zarba RL (1990) A general mass-conservative numerical solution for the unsaturated flow equation. Water Resources Research 26(7):1483–1496

Cox SJ, Weaire D, Hutzler S, Murphy J, Phelan R, Verbist G (2000) Applications and generalizations of the foam drainage equation. Proceedings of the Royal Society of London A: Mathematical, Physical and Engineering Sciences 456:2441–2464

Cuesta C, van Duijn CJ, Hulshof J (2000) Infiltration in porous media with dynamic capillary pressure: Travelling waves. European Journal of Applied Mathematics 11:381–397

van Duijn CJ, Mitra K, Pop IS (2018) Travelling wave solutions for the Richards equation incorporating non-equilibrium effects in the capillarity pressure. Nonlinear Analysis: Real World Applications 41:232–268

El Behi-Gornostaeva E, Mitra K, Schweizer B (2019) Traveling wave solutions for the Richards equation with hysteresis. IMA Journal of Applied Mathematics 84:797–812

Fredlund DG, Xing A (1994) Equations for the soil-water characteristic curve. Canadian Geotechnical Journal 31(4):521–532

van Genuchten MT (1980) A closed-form equation for predicting the hydraulic conductivity of unsaturated soils. Soil Science Society of America Journal 44(5):892–898

van Genuchten MT, Nielsen DR (1985) On describing and predicting the hydraulic properties of unsaturated soils. In: Annales Geophysicae, vol 3, pp 615–628

Grassia P, Mas-Hernández E, Shokri N, Cox SJ, Mishuris G, Rossen WR (2014) Analysis of a model for foam improved oil recovery. Journal of Fluid Mechanics 751:346–405

Koehler SA, Hilgenfeldt S, Stone HA (1999) Liquid flow through aqueous foams: The node-dominated foam drainage equation. Physical Review Letters 82(21):4232–4235

Koehler SA, Hilgenfeldt S, Stone HA (2000) A generalized view of foam drainage: Experiment and theory. Langmuir 16(15):6327–6341

Mitra K, van Duijn CJ (2019) Wetting fronts in unsaturated porous media: The combined case of hysteresis and dynamic capillary pressure. Nonlinear Analysis: Real World Applications 50:316–341

Morrow NR, Harris CC (1965) Capillary equilibrium in porous materials. Society of Petroleum Engineers Journal 5:15–24

Mualem Y (1976) A new model for predicting the hydraulic conductivity of unsaturated porous media. Water Resources Research 12(3):513–522

Or D, Assouline S (2011) The Drainage Foam Equation: An alternative to the Richards Equation for transient unsaturated flows. In: AGU Fall Meeting Abstracts

Or D, Assouline S (2013) The foam drainage equation for unsaturated flow in porous media. Water Resources Research 49(10):6258–6265

Philip JR (1957) The theory of Infiltration: 1. The Infiltration Equation and its solution. Soil Science 83(5):345–358

Richards LA (1931) Capillary conduction of liquids through porous mediums. Physics 1(5):318–333

Stankovich JM, Lockington DA (1995) Brooks-Corey and van Genuchten soil-water-retention models. Journal of Irrigation and Drainage Engineering 121(1):1–7

Verbist G, Weaire D (1994) A soluble model for foam drainage. EPL (Europhysics Letters) 26(8):631–634

Verbist G, Weaire D, Kraynik AM (1996) The foam drainage equation. Journal of Physics: Condensed Matter 8(21):3715–3731

Vogel T, Cislerova M (1988) On the reliability of unsaturated hydraulic conductivity calculated from the moisture retention curve. Transport in Porous Media 3(1):1–15

Weaire D, Phelan R (1996) The physics of foam. Journal of Physics: Condensed Matter 8(47):9519–9524

A Theoretical Basis for the Predictive Conductivity Models

This appendix outlines the basis for predictive conductivity models (PCM). Although we do not ultimately apply a PCM in our analysis, we include this appendix to demonstrate why a soil-water retention curve (SWRC) that goes to zero smoothly at high saturation is incompatible with convergence of a PCM hence the reason a PCM was not employed in our analysis. Conversely, we show why the SWRC (if it goes to zero at all at full saturation) must do so abruptly in order for the PCM to converge, and moreover why the PCM approaches unity abruptly at full saturation in that case. Full details of the theory presented in this section are given in Burdine (1953); Brooks and Corey (1964, 1966); Mualem (1976).

The reason why PCM have been developed in the first place is that the experimental determination of relative hydraulic conductivity (RHC) is often considered complicated and expensive (Or and Assouline, 2011). Thus, for many practical applications, it can be advantageous to attempt to determine RHC mathematically from SWRC data which are based on soil pore-size distribution. The more commonly used PCM (Burdine, 1953; Mualem, 1976) that link SWRC to RHC functions assume a simple pore geometry and link capillary properties of pores to RHC. However, as we will see, they also impose a constraint on the SWRC if the RHC is to converge.

A typical PCM leads to a general expression given as

$$K_r(\Theta) = \Theta^{\kappa} \left[\int_0^{\Theta} \frac{1}{H_+^{\delta}} \mathrm{d}\Theta \Big/ \int_0^1 \frac{1}{H_+^{\delta}} \mathrm{d}\Theta \right]^{\eta} \tag{A. 1}$$

where κ, δ, η are model parameters. It is found that $\kappa = 2$, $\delta = 2$, and $\eta = 1$ for the Burdine model (Burdine, 1953), and $\kappa = 1/2$, $\delta = 1$, and $\eta = 2$ for the Mualem model (Mualem, 1976). We focus on the derivation of the Mualem model.

A.1 Mualem's Predictive Conductivity Model

Mualem (1976) considers a homogeneous porous medium with a set of interconnected pores defined by their radius r, and a pore-water distribution function $f(r)\mathrm{d}r$. The contribution of filled pores of radii between r and $r + \mathrm{d}r$ to the volumetric moisture content θ (rescaled here as Θ) is

$$f(r)\mathrm{d}r = \mathrm{d}\Theta(r). \tag{A. 2}$$

Considering a porous slab of thickness Δx, the pore area distribution at the two slab sides is assumed to be identical. The probability $a(r,\rho)$ of a pore of size r to $r + \mathrm{d}r$ at location x encountering a pore of radius ρ to $\rho + \mathrm{d}\rho$ at $x + \Delta x$ is

$$a(r,\rho) = f(r) f(\rho)\, \mathrm{d}r\, \mathrm{d}\rho. \tag{A. 3}$$

More generally, the probability of connection for a pore of radius between r and $r+\mathrm{d}r$ to a pore of radius between ρ and $\rho+\mathrm{d}r$ may be given as

$$a(r,\rho) = G(r,\rho) f(r) f(\rho)\,\mathrm{d}r\,\mathrm{d}\rho, \tag{A. 4}$$

where the function $G(r,\rho)$ accounts for partial correlation between the pores r and ρ at a given moisture content Θ. In what follows, two pores in series with radius r and ρ respectively are replaced by a single equivalent pore radius R and it is assumed that $G(r,\rho)$ can be expressed as a function $G(R)$. To determine conductivity, this connection probability needs to be weighted by a local hydraulic conductivity for each equivalent pore.

Mualem (1976) considers a pair of capillary elements whose lengths are proportional to their radii to replace the pore configuration, and estimates the local hydraulic conductivity as proportional to $r\rho$ or more specifically as $T(r,\rho)r\rho$ where $T(r,\rho)$ is a correction due to tortuosity. Again, it is assumed that $T(r,\rho)$ can be expressed as $T(R)$ where R is a single equivalent radius. The term in $r\rho$ comes about as follows. Two pores in series (length l_r and l_ρ respectively) are replaced by a single equivalent pore (length L). The pressure drop across the equivalent pore is assumed to be the same as the total pressure drop along the two original pores in series. Since Poiseuille pressure drops scale as $(8/\pi)\mu QL/R^4$ (and μ is viscosity and Q is flow rate, which is the same in all cases), it follows

$$L/R^4 = l_r/r^4 + l_\rho/\rho^4. \tag{A. 5}$$

Moreover, since the volume of the equivalent pore is assumed to be the same as total volume of the two original pores, it follows that

$$LR^2 = l_r r^2 + l_\rho \rho^2. \tag{A. 6}$$

Significantly, the length of the equivalent pore need not be the same as the total length of the two original ones. Finally the aspect ratio of the pores is assumed fixed, hence

$$l_r/r = l_\rho/\rho. \tag{A. 7}$$

The above constitute 3 homogeneous linear equations (A. 5)–(A. 7) in 3 unknowns L, l_r and l_ρ. Non-trivial solutions only result if the determinant of the system of equations is zero. This provides a condition linking R to r and ρ, specifically

$$R = \sqrt{r\rho}. \tag{A. 8}$$

Taking the local hydraulic conductivity proportional to $r\rho$ as was suggested above is equivalent to taking the conductivity of equivalent pore properties to R^2 which is what is expected for a single pore. Solutions can now be obtained for l_r and l_ρ assuming L is given. It is necessary to fix the value of L since when the determinant vanishes, the equations are not all linearly independent.

$$l_r = Lr^2\rho/(r^3+\rho^3), \qquad l_\rho = Lr\rho^2/(r^3+\rho^3). \tag{A. 9}$$

Note that

$$l_r + l_\rho = Lr\rho(r+\rho)/(r^3+\rho^3) \tag{A. 10}$$

which is always smaller than L. Note however that the volume of the equivalent pore is the same as the sum of the volumes of the two original ones by construction. Once we have established the size of a single equivalent pore, we have also established the liquid saturation, since we consider that the medium is filled up to pores of a given size but no further. Supposing we can re-write the tortuosity and connectivity factors as functions of Θ (instead of in terms of r and ρ, or in terms of R), it follows that the hydraulic conductivity K is (assuming r_{min} and ρ_{min} are minimum sizes)

$$K \propto T(\Theta)G(\Theta)\int_{r_{min}}^{r} r f(r)\mathrm{d}r \int_{\rho_{min}}^{\rho} \rho f(\rho)\mathrm{d}\rho, \tag{A. 11}$$

and relative hydraulic conductivity is (assumng R_{min} and R_{max} are minimum and maximum sizes)

$$K_r(\Theta) = T(\Theta)G(\Theta)\left[\int_{R_{min}}^{R} r f(r)\,\mathrm{d}r \Big/ \int_{R_{min}}^{R_{max}} r f(r)\,\mathrm{d}r\right]^2. \tag{A. 12}$$

Here we have exploited the fact that the integrals over r and ρ are the same, and the denominator of equation (A. 12) is a normalisation condition. The important point here is that unless $f(r)$ decays quite rapidly as r becomes large (decaying faster than $1/r^2$), K does not converge, or equivalently the denominator of K_r diverges, making K_r itself tend to zero.

If too much volume is associated with the large pores, which only fill near saturation, effectively all the flow at saturation is dominated by transport through those large pores, and in relative terms, below saturation flow is negligible. In situations like that, we can expect to see large variations in conductivity between rock samples, since the presence of slightly different numbers of large pores in different samples may influence hydraulic conduction.

The tortuosity correction factor $T(\Theta)$ that is applied, and the connectivity correlation factor $G(\Theta)$ are assumed to be power-law functions of Θ, and are replaced by a single factor Θ^{κ}. Substituting $\kappa = 1/2$ (fit by Mualem (Mualem, 1976; Assouline, 2001) to 45 soil samples) within the that term, applying the capillary law relating pore radius to capillary head $r = C/H_+$ where C is a constant (independent of geometry), and using equation (A. 2), we obtain for equation (A. 12)

$$K_r(\Theta) = \Theta^{1/2}\left[\int_0^{\Theta}\frac{\mathrm{d}\Theta}{H_+}\bigg/\int_0^{1}\frac{\mathrm{d}\Theta}{H_+}\right]^2. \tag{A. 13}$$

As noted in the main text, there are convergence issues here if H_+ is too small for too large a fraction of the volume in the limit as $H_+ \to 0$. If, for example, $H_+ \approx |\mathrm{d}H_+/\mathrm{d}\Theta|_{\Theta=1}(1-\Theta)$ for some finite $|\mathrm{d}H_+/\mathrm{d}\Theta|_{\Theta=1}$, then $\int_0^1 \mathrm{d}\Theta/H_+$ diverges. As mentioned earlier, the issue is that there is now so much volume in large radius (small H_+) pores that almost all conduction occurs through large pores. A larger (i.e. singular) $|\mathrm{d}H_+/\mathrm{d}\Theta|$ resolves the issue by having less volume in such small H_+ pores. The SWRC selected by van Genuchten (van Genuchten, 1980) typically has for Θ close to 1

$$H_+ \approx ((1-\Theta)/m)^{1-m}; \qquad \Theta \approx (1 - mH_+^{1/(1-m)}), \tag{A. 14}$$

for some value $m < 1$ (typically with m close to 1 for sandstones, and m significantly less than 1 for loams). Here we recognise via equation (A. 2), that

$$f(r) = \frac{\mathrm{d}\Theta}{\mathrm{d}r} = \frac{\mathrm{d}\Theta}{\mathrm{d}H_+}\cdot\frac{\mathrm{d}H_+}{\mathrm{d}r}, \tag{A. 15}$$

and also recognise that (as alluded to earlier),

$$H_+ = \frac{C}{r}. \tag{A. 16}$$

It follows then that in the limit of large r (i.e. small H_+)

$$\begin{aligned} f(r) &\approx \frac{m}{(1-m)}H_+^{m/(1-m)}\cdot\frac{C}{r^2} \\ &\approx \frac{m}{(1-m)}\frac{C^{m/(1-m)}C}{r^{m/(1-m)}r^2} \\ &\approx \frac{m}{(1-m)}\frac{C^{1/(1-m)}}{r^{(2-m)/(1-m)}}. \end{aligned} \tag{A. 17}$$

Notice how this function decays in the large r limit. If m is close to 1 (e.g. sandstone), $f(r)$ decays very rapidly at large r, so there are comparatively few pores that are much larger than the sample average. If m is rather smaller than unity (e.g. loam), the population of pores that are significantly larger than the sample average increases. Certainly, the average pore size in loam tends to be much smaller than in sandstone but that effect is already accounted for in our dimensionless system. What we are considering here is not the average pore size, but rather the pore size distribution relative to that average. Note that in the limit as $m \to 0$, hence with a non-singular $H_+ \propto (1-\Theta)$, it follows via (A. 17) that $f(r)$ becomes proportional to r^{-2}, and (as noted earlier) the denominator of (A. 12) then fails to converge as $R_{max} \to \infty$. Yet again this demonstrates that there are now, in relative terms, so many large pores that almost all the flow is passing through them, so the (total) conductivity we compute is sensitive to what exactly the largest pore size R_{max} is. As $R_{max} \to \infty$, the hydraulic conductivity up to any finite pore size $R < R_{max}$ is then negligibly small compared to the conductivity through the very largest pores, so that relative conductivity K_r (considered only up to that finite pore size) tends to zero.

Assuming on the other hand that $0 < m < 1$ so that equation (A. 13) does indeed converge, notice however

$$\frac{\mathrm{d}K_r}{\mathrm{d}\Theta} \approx \frac{1}{2\Theta}K_r + \frac{2\Theta^{1/2}}{H_+}\int_0^{\Theta}\frac{\mathrm{d}\Theta}{H_+}\bigg/\left(\int_0^1\frac{\mathrm{d}\Theta}{H_+}\right)^2. \tag{A. 18}$$

The consequence of having $H_+ \to 0$ abruptly as $\Theta \to 1$, e.g. H_+ scaling as proportional to $(1-\Theta)^\alpha$ for some $0 < \alpha < 1$ with $\alpha = 1-m$ here (see equation (A. 14)), is that $\mathrm{d}K_r/\mathrm{d}\Theta$ also diverges as $(1-\Theta)^{-\alpha}$ in that same limit. A singular H_+ vs Θ relation leads to a convergent K_r vs Θ but *not* a convergent $\mathrm{d}K_r/\mathrm{d}\Theta$ vs Θ, at least in the PCM adopted here. The only way to keep $\mathrm{d}K_r/\mathrm{d}\Theta$ from diverging is to take $\alpha \to 0$, i.e. $m \to 1$. However that means according to (A. 14) that H_+ must stay non-zero as full saturation is approached. Returning to the case $0 < m < 1$ however, the value of $D_r(\Theta)$ predicted by the PCM meanwhile is divergent, since $D_r = K_r|\mathrm{d}H_+/\mathrm{d}\Theta|$ (van Genuchten, 1980), and since we require $\mathrm{d}H_+/\mathrm{d}\Theta$ to diverge in order to have a convergent K_r, it necessarily follows that D_r diverges.

In conclusion, using the predictive conductivity model PCM we have a choice between a system in which H_+ remains non-zero at full saturation (in which case K_r converges to unity at $\Theta \to 1$ with finite $\mathrm{d}K_r/\mathrm{d}\Theta$ there), or a system in which H_+ approaches zero smoothly at full saturation (in which case K_r is not well defined in the PCM, since conduction is dominated by the flow through the largest pores in the sample, hence is extremely sensitive to the particular sample), or else a system in which $H_+ \to 0$ and $K_r \to 1$ at full saturation, but necessarily with mild singularities in that limit (both $|\mathrm{d}H_+/\mathrm{d}\Theta|$ and $|\mathrm{d}K_r/\mathrm{d}\Theta|$ diverge at full saturation). In the main text, we have avoided with issue by abandoning the PCM.

B Appendix B

This appendix summarises some of the findings from Boakye-Ansah and Grassia (2021) regarding how travelling wave solutions of Richards equation behave when using the original van Genuchten (1980) soil material property functions. The relevant solutions are presented here for ease of comparison with those presented in the main text that use modified soil material property functions.

The profile of the travelling wave to Richards equation previously obtained within the limit of the special case we consider is

$$\frac{\mathrm{d}\xi}{\mathrm{d}\Theta} = \frac{D_r(\Theta)}{\Theta - K_r(\Theta)}, \tag{B. 1}$$

which is analogous to equation (14) (identical to equation (15)). In the case of equation (B. 1) above, the original D_r and K_r functions given by van Genuchten are used in its solution.

Near $\Theta \approx 1$,

$$D_r(\Theta) \approx \left|\frac{\mathrm{d}H_+}{\mathrm{d}\Theta}\right| \approx \frac{(1-m)}{m^{(1-m)}}(1-\Theta)^{-m}, \tag{B. 2}$$

is the approximation used which is the derivative of the original van Genuchten SWRC in the same limit (Boakye-Ansah and Grassia, 2021). The denominator of equation (B. 1) is also scaled as

$$\Theta - K_r \approx (1-K_r) - (1-\Theta). \tag{B. 3}$$

If $K_r \to 1$ abruptly as $\Theta \to 1$, then typically, $1-\Theta \ll 1-K_r$. As explained in Boakye-Ansah and Grassia (2021) moreover

$$1 - K_r \approx \frac{2}{m^m}(1-\Theta)^m. \tag{B. 4}$$

Hence,

$$\frac{\mathrm{d}\xi}{\mathrm{d}\Theta} \approx \frac{|\mathrm{d}H_+/\mathrm{d}\Theta|}{1-K_r(\Theta)}; \qquad \frac{\mathrm{d}\xi}{\mathrm{d}\Theta} \approx \frac{(1-m)}{2m^{1-2m}}(1-\Theta)^{-2m}, \tag{B. 5}$$

for which we obtain

$$\xi = c_0 + \frac{(1-m)m^{2m-1}}{2(2m-1)}(1-\Theta)^{1-2m}, \tag{B. 6}$$

where c_0 is an integration constant. Here we are primarily interested in m values $0.5 < m < 1$ so that $-1 < 1-2m < 0$. Note that this is a power law for ξ, hence it grows more rapidly than the logarithmic law discussed in the main text. We have expressed this in terms of a variable ξ rather than a rescaled variable $\hat{\xi}$ which was not used in Boakye-Ansah and Grassia (2021) owing to equation (B. 2) diverging in the $\Theta \to 1$ limit. However, for comparison we can convert from ξ to $\hat{\xi}$ by dividing through by the capped maximum value of $|\mathrm{d}H_+/\mathrm{d}\Theta|$ given in Table 1.